SIMULATION ASSISTED DESIGN FOR AN ADDITIVELY MANUFACTURED AUTOCLAVE TOOL ACCOUNTING FOR AN ANISOTROPIC EXPANSION

Ahmed Arabi Hassen[1], Alexander Lambert[1], John Lindahl[1], Dylan Hoskins[2], Chad Duty[1,2], Srdjan Simunovic[1], Charlie Chin[3], Victor Oancea[3], Lonnie Love[1], Vlastimil Kunc[1], and Seokpum Kim[1]

[1] Oak Ridge National Laboratory, Oak Ridge, TN 37830
[2] Mechanical, Aerospace and Biomedical Engineering, University of Tennessee, Knoxville, TN 37996
[3] Dassault Systèmes SIMULIA, Johnston, RI 02919

ABSTRACT

Carbon fiber reinforced polymer composites have been used in Big Area Additive Manufacturing (BAAM) to decrease the distortion during the printing process and increase functional stiffness. These materials are also important for additively manufactured autoclave tooling which expands when exposed to the high temperatures of the operational cycle, causing the dimensions of the mold to differ from the targeted design. Since the reinforcing fibers generally align during the extrusion process, the thermal expansion of the composite along the deposition direction is restrained by fibers, whereas the thermal expansion perpendicular to the bead is largely unconstrained. This leads to an anisotropic expansion of the material that is dependent upon the local deposition path, which may be tortuous and complex. To obtain an accurate final part geometry during the autoclave process, a computational prediction of the thermal expansion of a tool is required to account for the complex extrusion deposition directions. A multi-step approach is presented that accounts for (1) anisotropic thermal expansion of the extruded bead, (2) the complex deposition directions, and (3) internal geometry determined by slicing software. The thermal expansion coefficient in the deposition direction and perpendicular to the deposition direction were measured at multiple locations in the test specimen. A revised model geometry was generated to achieve the target dimensions when accounting for thermal expansion.

1. INTRODUCTION

Additive manufacturing (AM) techniques can provide short lead times with low manufacturing costs. Large scale AM technology in the last 5 years have shown great success for the fabrication of out-of-autoclave molds (lay-up tools) [1-5] and in-autoclave molds [6-8] for composite manufacturing. The autoclave molding technique is often used in composite manufacturing when high temperature or high pressure is required for curing. Because the technique provides dense

CAMX Conference Proceedings. Anaheim, California, September 23-26, 2019. CAMX – The Composites and Advanced Materials Expo

composites with a low void content, it is widely used for high-strength components [9]. During the autoclave cycle, the mold expands due to the elevated temperature and the dimensions of the molding surface at the composite molding temperature differs from the original design. For conventional molds made out of metallic substrates, such as Aluminum, Steel or Invar, the change in the dimension (mold growth) is isotropic and predictable. A predictable scaling function/factor can be applied in order to obtain a final composite part within the design tolerances. This scaling factor become especially problematic for molds made out of polymeric materials. The coefficient of thermal expansion (CTE) of polymers is generally much larger than that of metals. One approach to reduce the CTE is to reinforce the polymer with carbon fibers. The thermal expansion of carbon fibers is an order of magnitude smaller than that of polymers, and therefore, the overall expansion decreases if carbon fiber reinforced polymer is used instead of neat polymers [10]. On the other hand, adding fibers to the polymer during the extrusion process leads to anisotropic behavior of the print and, therefore, predicting the thermal and mechanical performance becomes more challenging. As material flows through a narrow nozzle during the deposition process, fibers in the deposited bead generally align in the deposition direction. The thermal expansion of the composite along the bead is restrained by fibers, whereas the thermal expansion perpendicular to the bead is largely unconstrained. This leads to a highly anisotropic material as depicted in Figure 1.

AM autoclave molds have a complex deposition path. If the direction of anisotropy is consistent throughout the entire mold, then a global expansion coefficient can be applied in each primary direction to achieve the target dimensions of the mold following expansion. However, for AM molds, the deposition path changes from one location to another location (Figure 2) and predicting the overall expansion becomes quite complicated. In this case, the direction of individual deposition paths must be considered in order to accurately predicate the overall mold expansion. In this paper, a framework is presented that accurately predicts the thermal and mechanical performances of AM molds with a complex toolpath and anisotropic properties.

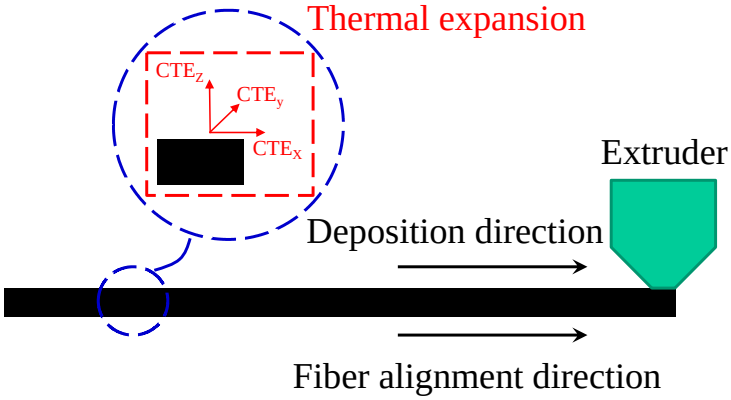

Figure 1: Anisotropic thermal expansion of a carbon fiber-reinforced polymer AM bead

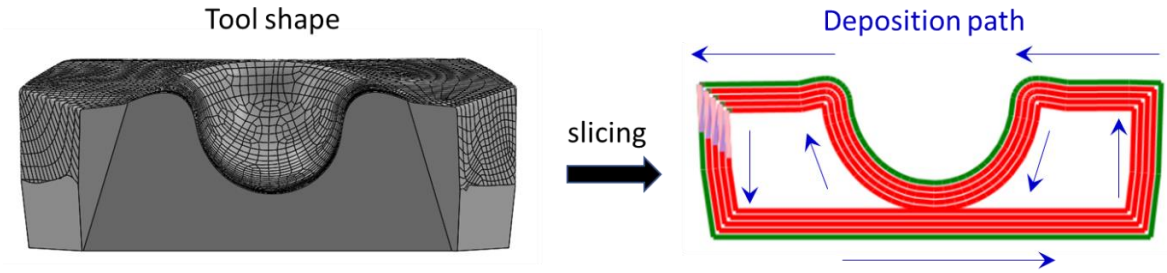

Figure 2: AM autoclave mold with complex deposition path resulting in complicated overall anisotropic thermal expansion

2. THERMAL EXPANSION MEASUREMENTS

Accurately predicting the thermal expansion via simulation depends on accurate measurements of thermal expansion properties. Therefore, the thermal expansion of several AM specimens were measured in x, y, and z directions, where the respective dimensions of the sample were 3 mm, 3 mm, and 10 mm. Samples were cut from a printed wall produced on the Big Area Additive Manufacturing (BAAM) system at Oak Ridge National Laboratory (ORNL). All cuts were preformed using a Buehler Isomet 1000 precision saw using a Buehler 15LC diamond wafering blade. The material used in this work was Polyphenylsulfone (PPSU) reinforced with 25% carbon fibers by weight. The CTE values were measured using a thermomechanical analysis (TMA) system. Since the fiber orientation in the bead closely follows the shear profile in the nozzle, a variation in the fiber orientation was observed through the thickness of the printed bead. Fibers near the outer perimeter of the bead experience higher shear flow and have a tendency to be more aligned, whereas the fibers nearer to the bead center are less aligned. Therefore, the thermal expansion at the periphery was expected to be lower than the thermal expansion near the center of the bead. As such, two specimens were prepared (Figure 3). The first was taken from the center of the bead (Location 1), and the second was taken from the bead to bead interface of the two beads (Location 2), which should be more highly aligned. It should be noted that, in this work, we have one sample for the z-directional CTE, as the specimen covers two-bead height (10 mm).

The specimens were dried in a Yamato ADP300C vacuum drying oven at 120 °C for 6 hours under 80 kPa vacuum. Specimens were then transferred to a desiccation chamber to cool to room temperature until TMA tests were performed. TMA testing was conducted using a Q400EM TMA with a macro-expansion probe from TA Instruments. In all directions, the CTE measurements followed the same experimental procedure. Initially the samples equilibrated to a temperature of 25 °C in the TMA. Next, the samples were heated at a rate of 5°C/min to 100 °C, cooled naturally to 25 °C, and then heated at a rate of 5 °C/min to 125 °C. The purpose of the 2nd heating cycle was to allow comparison between the two CTE measurements and ensure the data was repeatable. The average CTE over the temperature range was calculated using TA Instruments Universal Analysis software.

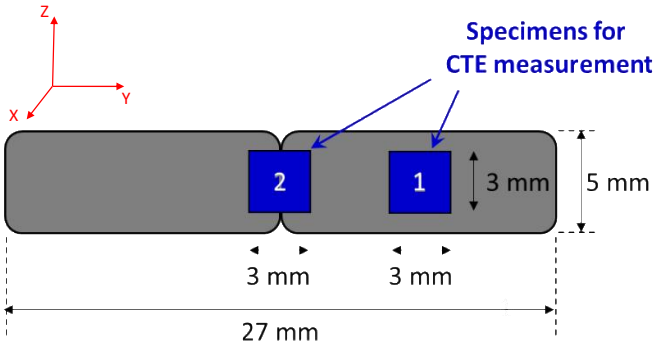

Figure 3: Schematic showing TMA samples size and location in deposited AM bead

An example TMA result is graphed in Figure 4 for sample 1 in the x direction. The temperature change with respect to time is plotted in red color in Figure 4(a), and the strain ($\Delta L/L_0$) with respect to time is plotted in blue color in Figure 4(a). The strain with respect to temperature is plotted in Figure 4(b). The expansion/contraction behavior of the sample was very consistent and linear during the heat-cool-heat cycles for all three primary directions. Therefore, the average CTE value was calculated as the slope of the line in Figure 4(b). The CTE values for each specimen are listed in Table 1 for the 3 primary directions indicated in Figure 1. As observed from Table 1, the CTE values in the x direction have the lowest values due to the highly oriented fibers in the deposition direction. The largest CTE value was in the z direction which is 700 % larger than of x directional CTE. Sample location in the bead highly affect the CTE results. It is noticed that for the x direction, CTE from sample 1 is twice of CTE from sample 2. This is attrbutided by the change of the fiber orientation within the deposited bead [11] where the periphery has more aligned fibers than the center of the printed bead. For the simulation framework develpoed in this work we have used the average value of the two tested locations (periphery and center) for the x-direction CTE.

Table 1: CTE in x, y, and z directions

Sample Direction	**Sample Location**	**CTE** $\boldsymbol{\mu m/(m \cdot K)}$	**CTE Average/Sample Direction** $\boldsymbol{\mu m/(m \cdot K)}$
x direction	1	14.4	10.84
x direction	2	7.28	
y direction	1	41.45	54.18
y direction	2	66.9	
z direction		74.7	74.7

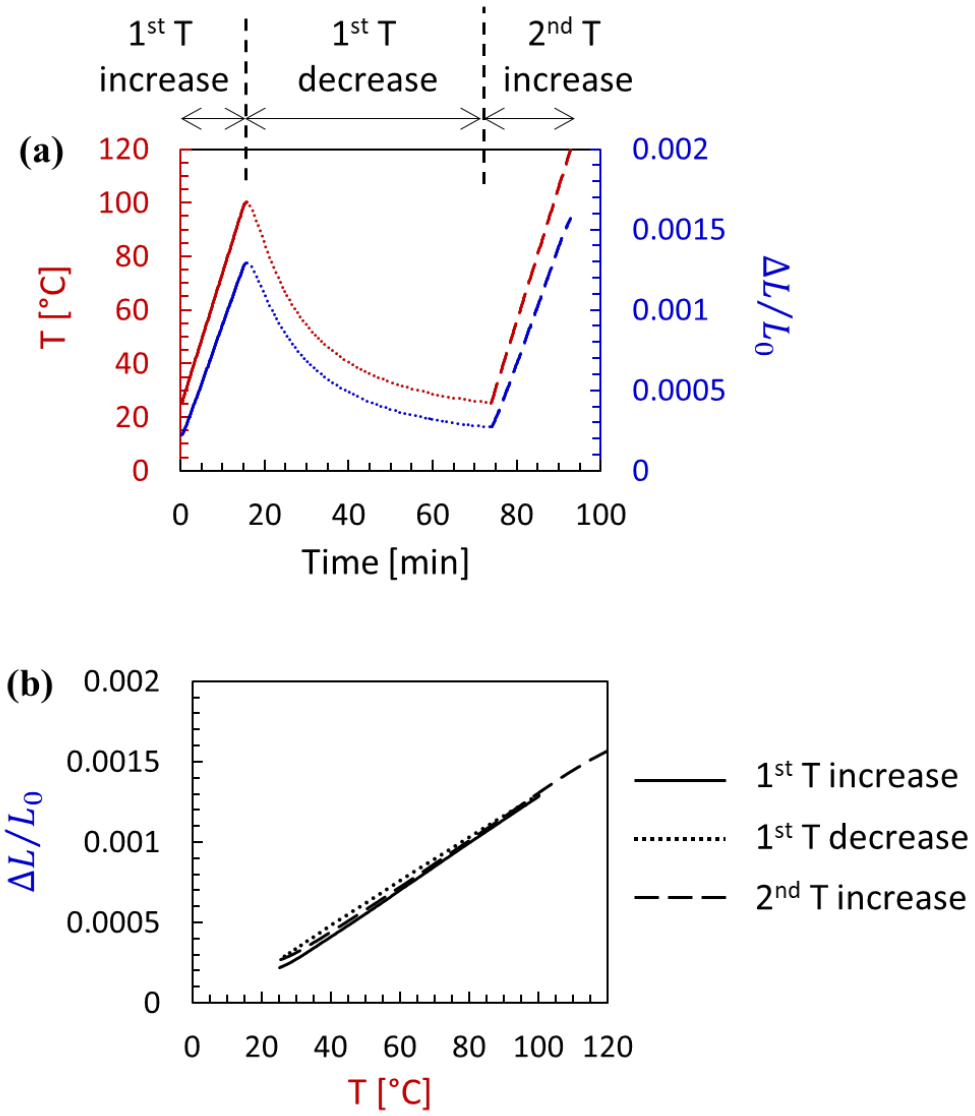

Figure 4: (a) Thermal expansion record from the TMA test for sample 1 in x-direction (b) Thermal expansion in for sample 1 in x-direction as a function of temperature.

3. SIMULATION

The expansion of an in-autoclave mold can be predicted via computational simulation using a finite element method (FEM). The simulation of the mold design is challenging for several reasons. First, the mold geometry to be printed is different from the original CAD design. The original CAD design is completely solid throughout the volume, whereas the printed design incorporates a fill pattern that is generated from Slicer. The slicer-generated design can vary depending on the Slicer settings as shown in Figure 5. To perform an accurate computational simulation, the slicer-generated design must be imported to FEM software. However, since Slicer does not directly communicate with the FEM software, the geometry had to be reconstructed based on a specified toolpath. The toolpath is the deposition path along which the extruder moves as determined by

Slicer. The second challenge is a non-uniform orientation of the anisotropic properties. The fibers in the printed bead were assumed to be generally aligned along the toolpath, which dictates the orientation of the anisotropic thermal/mechanical properties of the printed. Because the printed part consists of tortuous toolpath, the material property orientation in the simulation model must change as the toolpath direction changes.

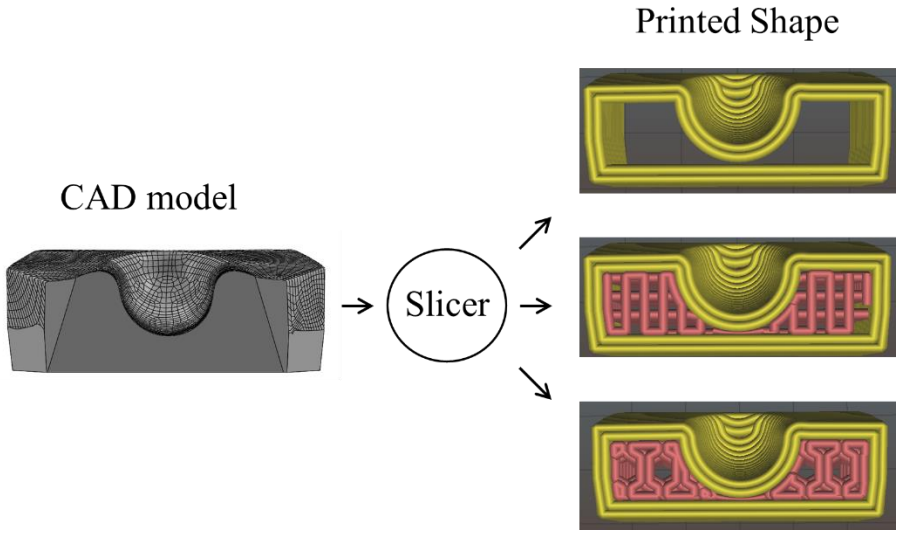

Figure 5: Slicer generates a toolpath with multiple options for a print shape that can be different from the original CAD geometry. The outmost surface geometry is the same, but the internal structure can vary depending on the Slicer settings.

The approach presented here for predicting the thermal expansion of an in-autoclave mold consists of the following steps. An internally solid model was created using CAD software (Step (a)). The STL formatted design file was imported into Slicer and converted into Gcode describing deposition toolpaths (Step (b)). The design file was also sent to FEM software for meshing (Step (c)), meaning that the entire geometry was spatially discretized into a large number of finite elements (FE). During the 3D-printing process simulation (Step (d)), the specific toolpath was mapped onto the FE mesh that was based on the original CAD file. In this step, only the discretized elements that were identified as lying on the toolpath were activated and the other elements are deactivated. At the same time, an orientation vector was assigned to each activated element to represent the toolpath directions (Step (d)). The activated elements and their property orientations were then used for the thermal expansion simulation (Step (e)). The overall flowchart for the simulation is shown in Figure 6.

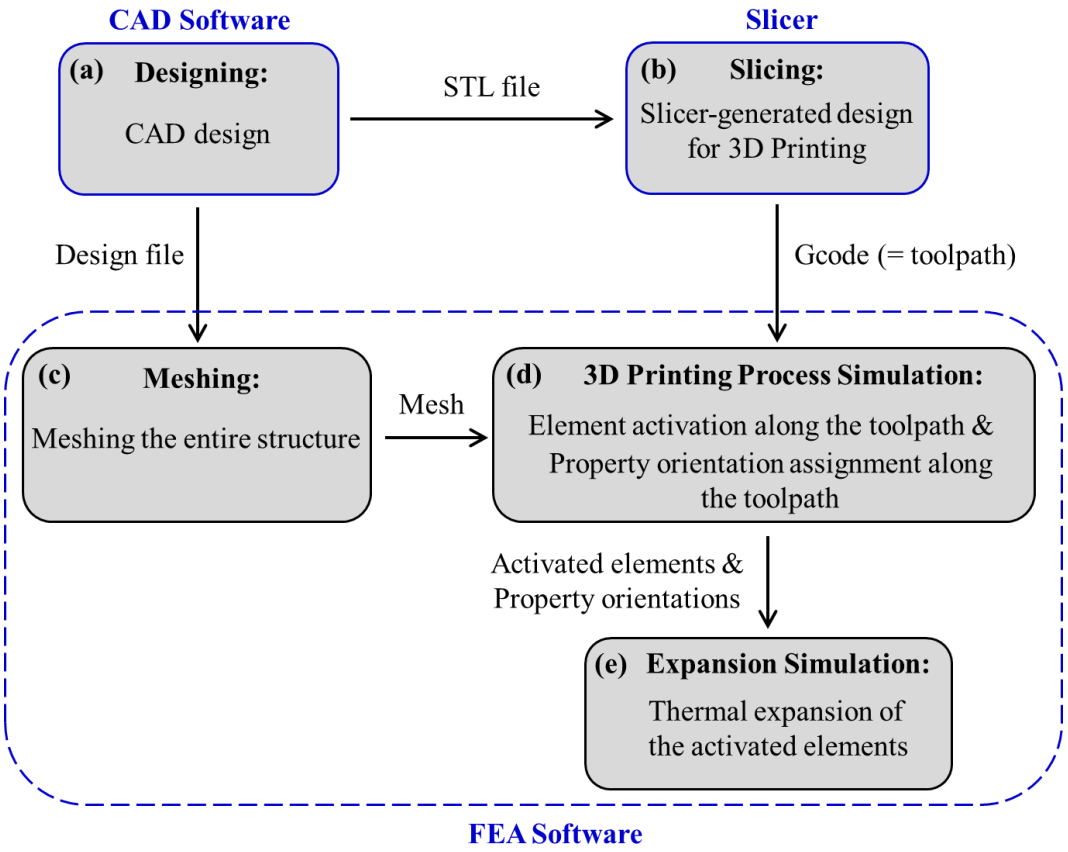

Figure 6: AM autoclave mold expansion prediction flowchart

After the thermal expansion simulation was performed, the deformation field of the outermost surface was used to reconstruct the target geometry. The reconstruction process accounted for the reversal direction of the deformation field after expansion and the open surface design that came from Slicer. The surface reconstruction in the reversal direction of the deformation field was then replaced by the deformation field from thermal shrinkage simulation (from high temperature to room temperature) instead of thermal expansion simulation (from room temperature to high temperature). Since the open surface design was originally generated from Slicer, the hollow internal space needed to be filled so that the design is internally fully solid. Once the target design was finalized following reconstruction of the surface, the design was used for 3D printing to obtain a near-net shape mold. The printed mold was then machined to obtain the final mold. The overall procedure after the simulation is shown in Figure 7.

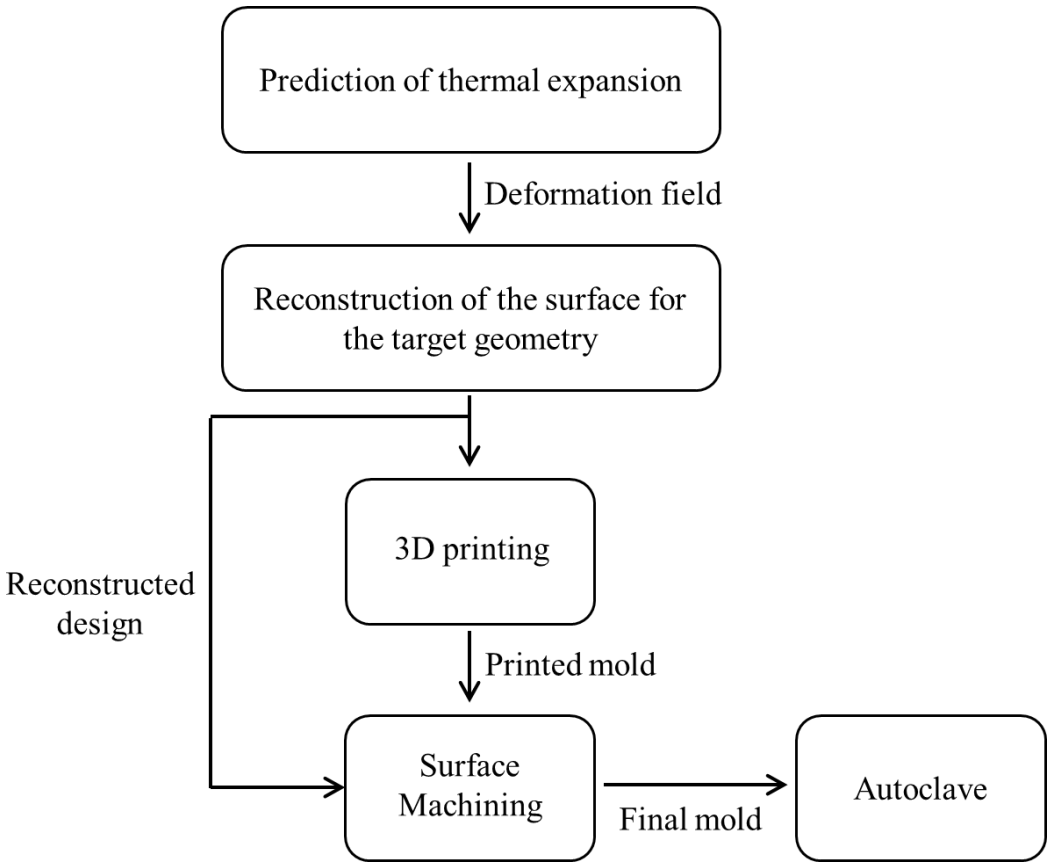

Figure 7: Flowchart showing the procedure to the final mold after the thermal expansion simulation step

This study performed the deformation prediction simulation as depicted in Figure 6. Abaqus was used for the FEM simulation, with the element activation and orientation assignment along the toolpath automatically accounted for in the solver. The additive simulation model was set up via the Abaqus additive manufacturing plugin, as detailed in Ref. [12]. The coefficients of thermal expansion in the x, y, and z directions were used in a thermal shrinkage simulation where the temperature varied from 177 °C to 30 °C. This study assumed that the amount of shrinkage during cooling was equal to the amount of expansion during heating between the same temperature change, which was confirmed experimentally in Figure 4(b). The displacement fields for the surface in the x, y, and z directions were obtained as shown in Figure 8. The displacement fields were then used for machining to obtain the desired surface dimensions such that the mold will expand to the correct dimensions in an autoclave.

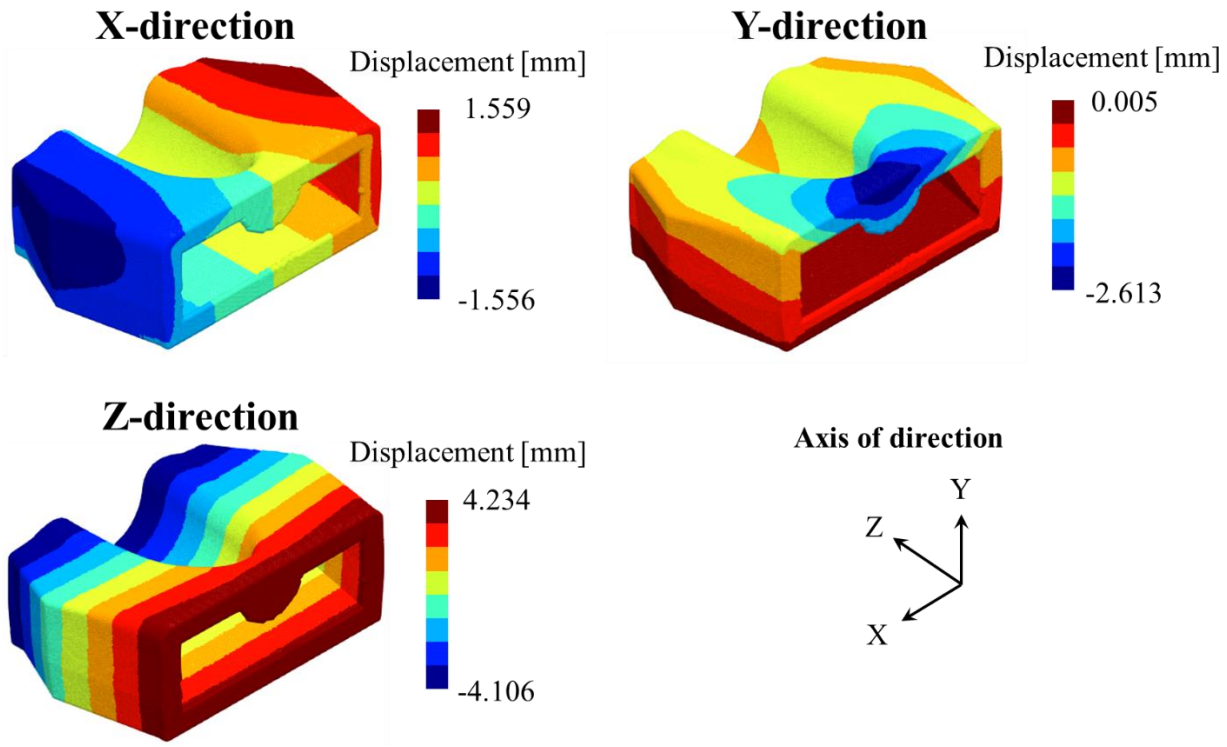

Figure 8: Displacement field of shrinkage in x, y, and z directions

4. CONCLUSIONS

A computational prediction of the thermal expansion of a tool was demonstrated in this study, accounting for the complex extrusion deposition directions in order to obtain an accurate geometry and dimensions during an autoclave process. A multi-step approach was presented that accounts for (1) anisotropic thermal expansion of the extruded bead, (2) the complex deposition directions, and (3) the internal geometry of the structure determined by slicing software. For accurate modeling parameters, thermal expansion coefficients in the deposition direction and perpendicular to the deposition direction were measured at multiple locations in the test specimen. The amount of expansion was subtracted from the original part design to obtain the new design with target dimensions.

ACKNOWLEDGEMENTS

Research sponsored by the U.S. Department of Energy, Office of Energy Efficiency and Renewable Energy, Industrial Technologies Program, under contract DE-AC05-00OR22725 with UT-Battelle, LLC.

5. REFERENCES

1. A.A. Hassen, R. Springfield, J. Lindahl, B. Post, L. Love, C. Duty, . . . , and V. Kunc. *The durability of large-scale additive manufacturing composite molds*. in *CAMX Conference Proceedings*. 2016. Anaheim, CA.
2. T.Z. Sudbury, R. Springfield, V. Kunc, and C. Duty, *An assessment of additive manufactured molds for hand-laid fiber reinforced composites.* The International Journal of Advanced Manufacturing Technology, 2017. **90**(5): p. 1659-1664.
3. B.K. Post, B. Richardson, R. Lind, L.J. Love, P. Lloyd, V. Kunc, . . . , and S. Nolet. *Big Area Additive Manufacturing Application in Wind Turbine Molds*. in *28th Annual International Solid Freeform Fabrication Symposium, August, in Austin, Texas, US*. 2017.
4. C.E. Duty, V. Kunc, B.S. Lokitz, and R.M. Springfield, *Evaluation of Additive Manufacturing for High Volume Composite Part Molds*. ORNL/TM-2017/122; CRADA/NFE-15-05793. Oak Ridge National Lab. 2017.
5. V. Kunc, A.A. Hassen, J. Lindahl, S. Kim, B. Post, and L. Love. *Large Scale Additively Manufactured Tooling For Composites.* in *Proceedings of 15th Japan International SAMPE Symposium and Exhibition*. 2017.
6. A.A. Hassen, J. Lindahl, X. Chen, B. Post, L. Love, and V. Kunc. *Additive manufacturing of composite tooling using high temperature thermoplastic materials*. in *SAMPE Conference Proceedings, Long Beach, CA, May*. 2016.
7. V. Kunc, J. Lindahl, R. Dinwiddie, B. Post, L. Love, M. Matlack, . . . , and A. Hassen. *Investigation of in-autoclave additive manufacturing composite tooling*. in *CAMX Conference Proceedings*. 2016. Anaheim, CA.
8. V. Kunc, C.E. Duty, J.M. Lindahl, and A.A. Hassen, *The Development of High Temperature Thermoplastic Composite Materials for Additive Manufactured Autoclave Tooling*. ORNL/TM-2017/437. NFE-16-06049. Oak Ridge National Lab. 2017.
9. F.Y.C. Boey and S.W. Lye, *Void reduction in autoclave processing of thermoset composites: Part 1: High pressure effects on void reduction.* Composites, 1992. **23**(4): p. 261-265.
10. L.J. Love, *Utility of Big Area Additive Manufacturing (BAAM) For The Rapid Manufacture of Customized Electric Vehicles*. ORNL/TM-2014/607. Oak Ridge National Lab. 2014.
11. B. Brenken, E. Barocio, A. Favaloro, V. Kunc, and R.B. Pipes, *Fused Filament Fabrication of Fiber-Reinforced Polymers: A Review.* Additive Manufacturing, 2018. **21**(May): p. 1-16.
12. Dassault Systèmes Simulia, *Abaqus/CAE Plug-in Utility for Additive Manufacturing Process Simulation*. [cited on Jun 6, 2019], Available from: https://onesearch.3dS.com/mashup-ui/page/document?q=docid:QA00000057533.